The Cryosphere Discuss., https://doi.org/10.5194/tc-2019-7
Manuscript under review for journal The Cryosphere
Discussion started: 29 January 2019

The Cryosphere Discussions
Open Access
EGU

Simulated retreat of Jakobshavn Isbræ during the 21st century

Xiaoran Guo[1], Liyun Zhao[1], Rupert Gladstone[2], Sainan Sun[3], John C. Moore[1,2,4]
[1]College of Global Change and Earth System Science, Beijing Normal University, Beijing 100875, China
[2]Arctic Centre, University of Lapland, P.O. Box 122, 96101 Rovaniemi, Finland
[3]Laboratoire de Glaciologie, Université libre de Bruxelles, Brussels, Belgium
[4]CAS Center for Excellence in Tibetan Plateau Earth Sciences, Beijing 100101, China

Correspondence to: John C. Moore (john.moore.bnu@gmail.com)

Abstract

The early in the 21st century retreat of Jakobshavn Isbræ, one of Greenland's largest outlet glaciers, into its over-deepened bedrock trough was accompanied by acceleration to unprecedented ice-stream speeds. Such dramatic changes suggested the possibility of substantial mass loss over the rest of this century. Using a three-dimensional ice-sheet model with parameterizations to represent the effects of ice mélange buttressing, crevasse-depth-based calving and submarine melting, we can reproduce its recent evolution. The model can accurately replicate its inter-annual variations in grounding line and terminus position, including new modes of seasonal fluctuations that emerged after arriving at the over-deepened basin and the disappearance of a persistent floating ice shelf. The shear margin induced decreases in ice viscosity we simulate are particularly important in reproducing the large observed inter-annual changes in terminus velocity. We use this model to project Jakobshavn's evolution over this century when forced by the IPCC RCP4.5 climate scenario and simulated by ocean temperatures from 7 Earth System Models along with surface runoff derived from RACMO. In our simulations, Jakobshavn's grounding line continues to retreat ~ 18.5 km by

The Cryosphere Discuss., https://doi.org/10.5194/tc-2019-7
Manuscript under review for journal The Cryosphere
Discussion started: 29 January 2019

the end of this century with total mass loss of ~ 2030 Gt (5.6 mm sea-level-rise equivalent). Despite the relative success of the model in simulating the recent behavior of the glacier, the model does not simulate winter calving events that have become relatively more important.

1 Introduction

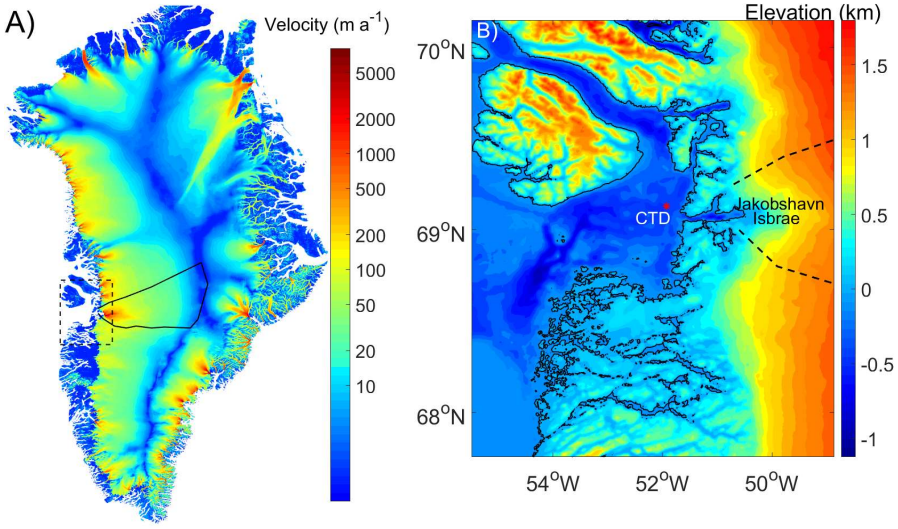

Figure 1. A) Greenland ice sheet flow speeds from Joughin et al. (2018), with the Jakobshavn drainage basin outlined by the solid black line and the area shown in panel B by the dashed box. B) Ilulissat Fjord and Disko Bay bathymetry from Jakobsson et al. (2012), with the CTD (Conductivity Temperature Depth) site used for ocean temperature here marked by the red star.

Jakobshavn Isbræ (Fig. 1) is Greenland's largest and fastest outlet glacier, with speeds of up to 17 km a^{-1} (Joughin et al., 2014). Jakobshavn Isbræ drains ~ 6.5 % of the Greenland Ice sheet (Krabill et al., 2000), and it alone contributed ~ 1 mm to global sea-level rise between 2000 and 2011 (Howat et al., 2011). Since 1997, measurements indicate that the water entering Ilulissat Fjord where Jakobshavn Isbræ terminates, is about 1.1 ºC warmer than it was during 1987-1991 (Holland et al., 2008). This rise in water temperature coincided with the onset of dramatic thinning, speedup and

retreat of Jakobshavn Isbræ. By 2003 its velocity near the grounding line had reached ~ 12.6 km a^{-1}, more than double that of 1992, and the floating ice mélange in the fjord had disintegrated (Joughin et al., 2004). From 2005 to 2007, as it retreated inland, seasonal fluctuations in velocity 4 km inland from the calving front amounted to ± 1 km a^{-1}. The winter slowdowns and summer accelerations occurred in tandem with the calving front winter advance and summer retreat. By 2012 the seasonal velocity fluctuations 4 km upstream from the calving front was nearly ± 8 km a^{-1} and the grounding line of Jakobshavn Isbræ had reached the bottom of a sub-glacial bedrock trough after years of down-slope migration (Joughin et al., 2014).

Before 1997, Jakobshavn possessed a ~ 15 km long floating ice mélange in front of its terminus ice cliff and experienced submarine melting on its ice-ocean interface (Amundson et al., 2010). After 1998 the terminus became more crevassed, coinciding with acceleration of the glacier, implying that weakened buttressing had triggered its dramatic speed-up. A thinning rate of 230 ± 50 m a^{-1} between the summers of 1984 and 1985 was deduced from photogrammetric surveys, mostly due to submarine melting (Motyka et al., 2011). The floating tongue thickened during the mid-1990s followed by progressive thinning after 1997 (Motyka et al., 2011). From 1997 to 2008, the average ocean temperature was 1.1°C higher than during the period 1980 – 1991, which raised its thinning rate substantially, affecting the whole ice mélange, and the ice shelf eventually collapsed in 2003. Many lines of evidence suggest that warm water was responsible for the submarine melting beneath the ice mélange and ice-shelf, brought by a buoyancy-driven, overturning circulation in Ilulissat fjord (Gladish et al., 2015).

Jakobshavn, in common with most outlet glaciers in Greenland, flows through a narrow, deeply incised bedrock trough at a far faster rate than the ice surrounding it (Joughin et al., 2010). Gravity surveys suggest a deep layer of soft till underlies much of the Jakobshavn trough (Block and Bell,

2011). This soft bed provides almost no resistance to ice flow and basal shear stress maps show that most of the gravitational driving force on the glacier is balanced by lateral drag (Shapero et al., 2016).

Basal drag decreased from 1995 to 2006 (Habermann et al., 2013), possibly due to fast thinning that reduced the effective pressure, that is the ice overburden minus water pressure, at the bed. The effective pressure distribution under the glacier is important to basal drag and must be zero at the grounding line as it begins to float. Several sliding parameterizations (also termed sliding relations or sliding laws) have been used in the literature that assume basal drag depends on sliding speed (so-called Weertman sliding), or on effective pressure (Schoof, 2010; Gagliardini et al., 2014). Tsai et al. (2015) introduced a combined Weertman and Coulomb sliding law based on effective pressures with a boundary layer at the grounding line; this has a higher scaling of ice flux with grounding-line thickness compared with the Weertman. However, in the Jakobshavn case, both Weertman and Coulomb sliding produce very similar fluxes because the basal shear stresses along the main trough are typically only 2 % of the driving force.

Simulations using a flow-band model with a crevasse-depth-based calving parameterization (Vieli et al., 2011) demonstrated that loss of buttressing from the disintegration of its floating ice mélange or enhanced submarine melting could have triggered the dramatic changes seen in Jakobshavn Isbræ at the end of the 20th century. Later work (Muresan et al., 2016), using a simple calving model with dependence on the strain field at the terminus was able to reproduce the inter-annual retreat of Jakobshavn Isbræ until 2009, when the terminus arrived at the beginning of the reverse sloping bed. But retreat after 2010 was not captured by their model, and neither was the seasonal fluctuation in terminus position.

In this paper we use a three-dimensional ice-flow model with a treatment of calving that successfully

The Cryosphere Discuss., https://doi.org/10.5194/tc-2019-7
Manuscript under review for journal The Cryosphere
Discussion started: 29 January 2019

tracks the seasonal terminus position and its retreat into the over-deepened basin. We use historic observations of ocean temperature as forcing and ice tongue thinning rate to scale submarine melting rates for our model and thence make future projections. Our aim is to track the evolution of Jakobshavn Isbræ through the 21st century under a specific climate forcing scenario. In Section 2 we describe the approach and calibration of our model, Section 3 shows the simulations for the period to 2100 under the IPCC RCP4.5 scenario (Moss et al., 2010), Section 4 is a discussion of our method with reference to other studies and suggestions for improvements, and we conclude in Section 5.

2 Methods and data

2.1 Ice sheet model

We model Jakobshavn Isbræ using the BISICLES continuum ice sheet dynamics model that is based on the vertically integrated stress balance formulation of Schoof and Hindmarsh (2010), which treats longitudinal and lateral stresses as depth-independent, but allows for vertical shear in the nonlinear rheology (Cornford et al., 2013). BISICLES is particularly useful for Jakobshavn Isbræ as it uses block-structured finite volume discretization with adaptive mesh refinement (Cornford et al., 2013) allowing for high resolution modeling of critical sections of the glacier. Jakobshavn Isbræ is fed by a ~ 400 km long and extensive drainage basin (Fig. 1), but the fast flow area is only around 10 km in width.

We assume Jakobshavn Isbræ to be in hydrostatic equilibrium, thus the upper surface elevation s is

$$s = \max\left[h + b, \left(1 - \frac{\rho_i}{\rho_w}\right)h\right], \quad (1)$$

The Cryosphere Discuss., https://doi.org/10.5194/tc-2019-7
Manuscript under review for journal The Cryosphere
Discussion started: 29 January 2019

where ρ_i and ρ_w are the densities of ice and ocean water, h is ice thickness and b is bedrock elevation relative to sea level. The ice thickness evolves in time as

$$\frac{\partial h}{\partial t} + \nabla \cdot [\boldsymbol{u}h] = M_s - M_b, \quad (2)$$

where M_s, M_b are surface mass balance (SMB) and submarine melt rate respectively and $\boldsymbol{u}$ is the depth-independent horizontal velocity. No basal melting over the grounded area is allowed. The velocity $\boldsymbol{u}$ satisfies an approximate stress balance equation

$$\nabla \cdot [\phi h\bar{\mu}(2\dot{\boldsymbol{\epsilon}} + 2\mathrm{tr}(\dot{\boldsymbol{\epsilon}})\mathbf{I})] - \boldsymbol{\tau}^b = \rho_i g h \nabla s, \quad (3)$$

where $\mathbf{I}$ is the identity tensor, s is the ice surface elevation, g is the acceleration due to gravity, $\dot{\boldsymbol{\epsilon}}$ is the horizontal strain-rate tensor defined by

$$\dot{\boldsymbol{\epsilon}} = \frac{1}{2}[\nabla \boldsymbol{u} + (\nabla \boldsymbol{u})^{\mathrm{T}}], \quad (4)$$

and $\boldsymbol{\tau}^b$ is the basal shear stress. The vertically integrated effective viscosity $\phi h\bar{\mu}$ is given by

$$\phi h\bar{\mu}(x, y) = \phi \int_{s-h}^{s} \mu(x, y, z)\mathrm{d}z, \quad (5)$$

where the vertically varying effective viscosity μ includes a contribution from vertical shear and satisfies

$$2\mu A(T)(4\mu^2\dot{\boldsymbol{\epsilon}}^2 + |\rho_i g(s - z)\nabla s|^2)^{(n-1)/2} = 1, \quad (6)$$

where n is the flow rate exponent, set to 3 in the current study, and $A(T)$ is the rate factor, dependent on the ice temperature T through an Arrhenius law (Cuffey and Paterson, 2010). ϕ is a stiffening factor estimated by solving an inverse problem (Cornford et al., 2015) using measured surface velocities.

The Cryosphere Discuss., https://doi.org/10.5194/tc-2019-7
Manuscript under review for journal The Cryosphere
Discussion started: 29 January 2019

We use a viscous Weertman sliding relation to define the basal friction:

$$\boldsymbol{\tau}^b = \begin{cases} -C|\boldsymbol{u}|^{m-1}\boldsymbol{u} & \text{if } \frac{\rho_i}{\rho_w} h > -b \\ 0 & \text{otherwise} \end{cases}, \quad (7)$$

and here we assume a linear relation taking m=1. The basal traction coefficient C(x, y) is estimated simultaneously with the stiffening factor ϕ by solving the inverse problem. C and ϕ are adjusted iteratively to reduce the misfit with a set of 2010 surface velocity observations (Joughin et al. 2010). We hold the fields C and ϕ constant over time throughout our simulations, although they must actually change as the glacier retreats.

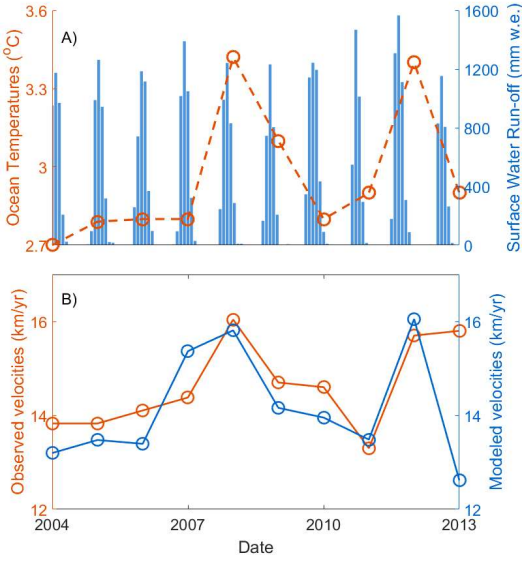

Figure 2. A) Time series of ~300 m deep ocean temperature (red) from http://ocean.ices.dk/HydChem/ near the mouth of Ilulissat fjord. Blue bars are simulated monthly surface water run-off from the MAR regional surface mass and energy balance model (Alexander et al. 2016). B) Measured ice front annual mean ice flow speeds (red) from Joughin et al. (2010), compared with our modeled speeds (blue).

The Cryosphere Discuss., https://doi.org/10.5194/tc-2019-7
Manuscript under review for journal The Cryosphere
Discussion started: 29 January 2019

2.2 Climate Forcing

We use ocean temperatures collected from a CTD site close to the mouth of Ilulissat fjord (Fig. 1) as an approximation of ocean temperatures near the glacier grounding line. A comprehensive study focusing on ocean circulation within Ilulissat fjord validated this approximation (Gladish et al. 2015). A positive correlation ($r=0.74$, $p<0.05$) exists between deep ocean temperatures and flow speed near the terminus of Jakobshavn Isbrae (Fig. 2) from 2004 onwards. There is no significant correlation prior to 2004, the floating ice tongue period. As a working hypothesis we assume that the correlation since 2004 reflects the effects of the sea ice and iceberg mélange in the fjord on the flow speed near the terminus: a warmer ocean reduces mélange thickness and therefore buttressing. There appears to be no lag between the glacier acceleration and change in deep ocean temperature, suggesting mélange response times are faster than 1 year. When the floating ice tongue was present lags in the system were likely longer, accounting for the lack of correlation between ocean temperatures and glacier flow speed prior to 2004. It is also possible that ocean temperatures reflect changes in surface runoff and basal lubrication for sliding, but we consider that the runoff more strongly affects calving mechanisms as discussed later. We therefore modify the driving force (Eq. 3) on the grid cells next to the calving front by multiplying by a factor α (tuned value shown by Eq. 9 that is linearly related to ocean temperature (T) as a means of representing the buttressing effects of the ice mélange in the fjord.

$$\nabla \cdot [\phi h \bar{\mu} (2\dot{\boldsymbol{\epsilon}} + 2\mathrm{tr}(\dot{\boldsymbol{\epsilon}})\mathbf{I})] + \boldsymbol{\tau}^b = \alpha \cdot \rho_i g h \nabla s, \quad (8)$$

$$\alpha = 0.82 + 0.111 \cdot T, \quad (9)$$

We use a crevasse based calving parameterization (Benn et al., 2007; Nick et al., 2011) that calves ice where the crevasse penetration depth (D_s) is greater than upper surface elevation. D_s is defined

as

$$D_s = \frac{S}{g \cdot \rho_i} + \frac{\rho_w}{\rho_i} \cdot \blacklozenge \cdot \beta, \quad (10)$$

where S is the magnitude of extensional stress, $\blacklozenge$ is surface water run-off, and β is a tuning scalar. We estimate runoff from the 25 km resolution regional climate model, MAR, (Alexander et al. 2016), driven by the ERA-Interim reanalysis (Dee et al., 2011).

We characterize submarine melting as a linear function of ocean forcing

$$M_b = \gamma T_f, \quad (11)$$

where T_f is the far field ocean forcing temperature, taken in Disko Bay (CTD in Fig. 1), relative to pressure melting temperature under the ice shelf. We derive γ from the 1985 observed submarine melt rate of 1 ± 0.2 m day^{-1} beneath the floating ice mélange of Jakobshavn Isbræ, when Disko Bay ocean temperatures were 4.2°C warmer than the pressure melting point at the bottom of the floating ice shelf (Motyka et al. 2011). We test the sensitivity of the modeled glacier to uncertainty in submarine melt rate in section 2.4.

We force Jakobshavn Isbræ in the 21st century using SMB and run-off from the 11 km resolution RACMO model (Van Angelen et al., 2013) driven by the RCP4.5 scenario (Moss et al. 2010). The run-off values are averaged over the nine grid points nearest to the terminus of Jakobshavn (69.1°N, 50.0°W). The RACMO simulation was forced by the HadGEM2-ES Earth system model (Collins et al., 2011), as this climate model was found to be the most realistic for present-day simulations of the Greenland ice sheet (Van Angelen et al., 2013). Ocean forcing should relate to temperatures off the continental shelf close to the fjord mouth. Cowton et al. (2018) achieved success in simulating the terminus position and yearly variability of 10 glaciers along the east coast of Greenland using

mean 200-400 m depth temperatures from reanalysis data. For consistency with the RACMO results, we use deep ocean temperatures at ~ 300 m depth from the 0.83°×1° resolution HadGEM2-ES driven by the RCP 4.5 climate scenario from 2005 to 2100 at the 3 closest grids point to Disko Bay. We also compare this with results from 7 other climate model simulations of RCP4.5: HadGEM2-ES (Collin et al., 2011), BNU-ESM (Ji et al., 2014), MIROC-ESM (Watanabe et al., 2011), IPSL-CM5A-LR (Dufresne et al., 2013), CSIRO-Mk3L-1-2 (Gordon et al., 2002), NorESM1-M (Bentsen et al., 2012) and MPI-ESM-LR (Giorgetta et al., 2013).

2.3 Initialization Procedure

As we are interested in high resolution simulations and validating our model parameterizations with observations over the last 2 decades, we take care to initialize the model as accurately as possible. Detailed bedrock topography and ice thickness data in the year 2009 come from Gogineni et al. (2012). In 2004 the floating ice shelf disintegrated, making it a convenient starting point for simulations since we might expect the system to respond differently to forcing when there was a floating ice shelf compared with the situation of ocean forcing along a near-vertical ice cliff. This is consistent with the observed good correlation between ocean temperature and flow speed after 2004 but not before. The aim of this initialization was provide a state rather similar to 2004, that is barely retreating on inter-annual scales (Joughin et al., 2010) and small changes of annual mean velocity in the following 3 years. Therefore

The Cryosphere Discuss., https://doi.org/10.5194/tc-2019-7
Manuscript under review for journal The Cryosphere
Discussion started: 29 January 2019

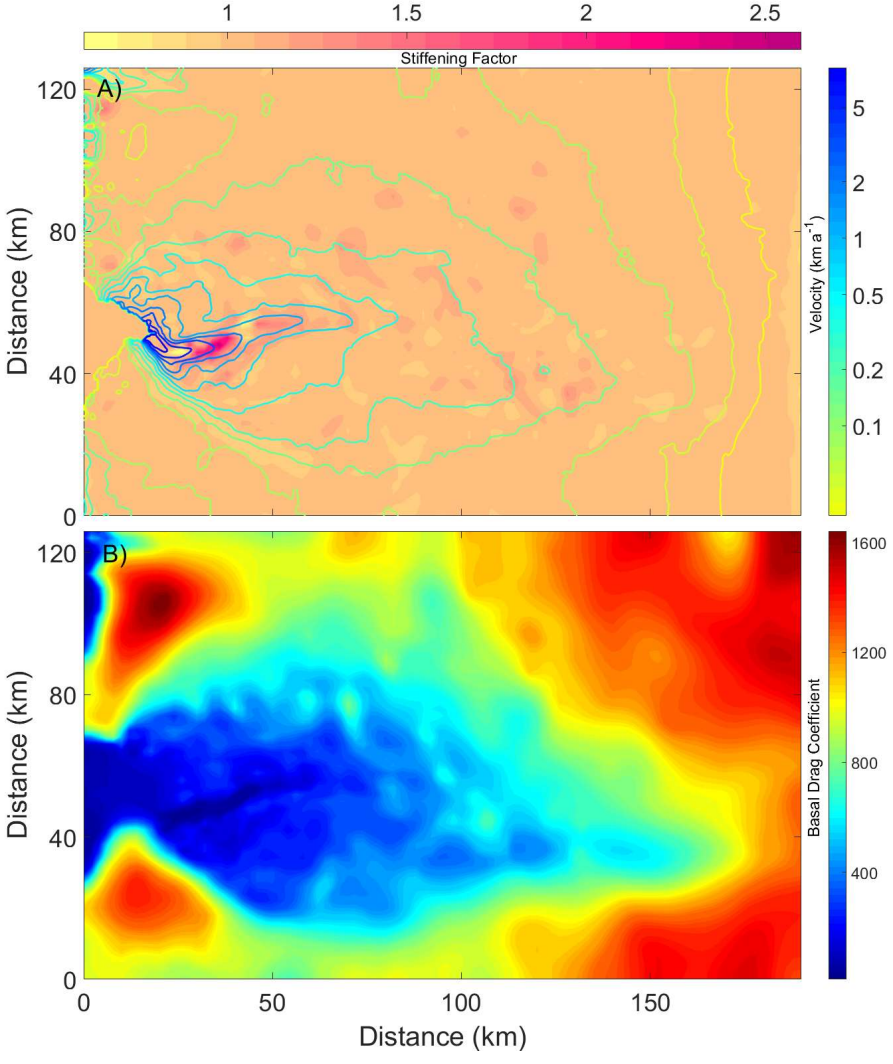

Figure 3. (A) Stiffening factor Φ (Eq. 3) and (B) basal traction coefficient C (Eq. 7) over the computational domain from solving the inverse problem. Contour lines in panel A show the modeled velocity (logarithmic scale).

1) We solved the inverse problem for basal conditions (Eq. 7) and stiffening factor using 2010 velocities (Joughin et al., 2010) and 2009 geometry (Gogineni et al., 2012). Our friction

coefficient field is shown in Fig. 3.

2) We made an initial guess for β (Eq. 10) based on short (less than one decade) transient simulations incorporating calving but not SMB or ice shelf melt forcing, starting from our inverted model state from step 1 above. This was forced by seasonal repetitions of runoff from MAR for the year 2010.

3) Starting from the inversion of step 1 and using β (Eq. 10) from step 2, we let the model glacier evolve freely without calving and with zero SMB and with sub-shelf melting forced by repeating the observed 2004 ocean temperature for 11 years (that means the coefficient γ in Eq. 11 was set to be 1) until its surface elevation profile was similar to the known profile of 1998 (Bamber et al. 2001).

4) We carried out several 10-year simulations with β gradually decreased from its initial value given by step 2, to 45% of this value. These simulations were forced by repeatedly applying the 2004 seasonal climate forcing. From these, we selected the β that best allowed Jakobshavn Isbræ to reach a stable state by the 8th year (changes in the 9th and 10th years of simulations were negligible) such that its calving front position closest to that observed in 2004. The best β here is 53% of its value from step 2. This is our best guess for the 2004 state, but there are no thickness data available for 2004. Notice that the front positions and May front velocities from 2004-2006 are stable (Figs 2 and 3), suggesting that the glacier was reasonably close to steady state. This also makes 2004 a good time from which to start transient simulations.

Basal friction coefficient values downstream of the 2010 grounding line were set equal to that in the nearest 2010 grounded location. This was necessary because steps 2, 3 and 4 involved

The Cryosphere Discuss., https://doi.org/10.5194/tc-2019-7
Manuscript under review for journal The Cryosphere
Discussion started: 29 January 2019

grounding line advance beyond the region for which basal friction coefficients had been inferred. The geometry after this spin up procedure, and the friction coefficient and stiffening factor distribution from the inversion in step 1 were used as the initial condition for model calibration.

2.4 Model calibration

There are three essential parameters in the model, α, β and γ representing mélange buttressing, crevasse depth sensitivity to surface runoff, and shelf melt sensitivity to ocean temperatures. In the initialization, we fix γ to be 1. Therefore, we performed a suite of about 50 simulations to tune the parameters α and β with fixed γ=1. Our target was to best reproduce Jakobshavn Isbræ's calving front position and surface velocity evolution for the 10 year period 2004-2013. Reproducing the total distance of retreat and the temporary stable state after 2012 were secondary desirable features to match.

Because only within a small range of β will modeled retreats make sense, firstly we estimate reasonable range of β when hold α=1.0, γ=1.0. Secondly, we explore the parameter space centered by (α=1.0, β=0.06), which come from estimations above, to match observed retreats and general velocities neglecting the inter-annual variations. The parameter space tested here is (1.0±0.25, 0.06±0.01). As the discussion above, we further assume $\alpha = \alpha_1 + \alpha_2 T$, i.e., linearly related to deep ocean temperature. With velocity depending on ocean temperature, degree of freedom of our parameter space grow to three, which are α_1, α_2, β. However, we find β and α_2 behave quite independently within the small β range estimated so far, which allow us finally reach a set of parameters that can accurately reproduce both the total retreats and the velocity variations including inter-annual fluctuation. The tuning was implemented manually. The best set of parameters are

245 α_1=0.82, α_2=0.111 and β=0.0638, as shown in Eq. 9.

246 We explore the glacier's sensitivity to two types of boundary perturbations. They are ice mélange
247 buttressing effect (defined by α) and submarine melting (defined by γ). We scaled submarine melt
248 rates by multiplying γ by values from 0.8-1.2, based on the range of the observation uncertainty in
249 melt of ~ 20% (Motyka et al. 2011). Also we varied α by multiplying by factors from 0.91 to 1.25
250 to represent different buttressing strengths (Eq. 8). These multiplication factors were varied
251 systematically with typical intervals of 0.1 and 0.03 respectively for the γ and α factors. We
252 calculated the following relative mismatches defined as (model-observations)/observations for each
253 simulation (shown in Fig 4):

254 1. Total calving front retreat from 2004-2013

255 2. Annual mean front velocities

256 3. Vector sum of 1) and 2)

257 We used β (Eq. 10) from our optimal set of parameters. Our optimal value for α is such that a
258 20% rise of its value does not affect modeled retreat when β and γ are kept to be their optimal
259 values (Fig. 4 A).

The Cryosphere Discuss., https://doi.org/10.5194/tc-2019-7
Manuscript under review for journal The Cryosphere
Discussion started: 29 January 2019

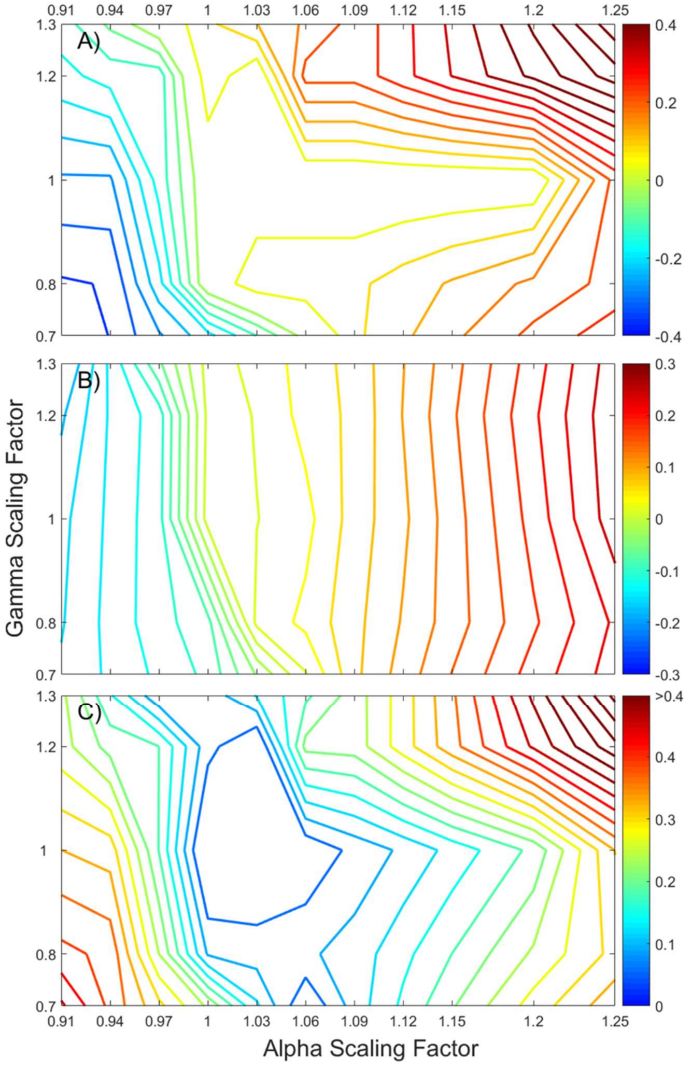

Figure 4. Relative mismatches defined as (model-observed)/observed for A) total calving front retreat, B) average of annual mean front velocity during 2004-2013, C) the vector sum of mismatches in panels A and B, $\sqrt{(A^2+B^2)}$ in our 2-D parameter space (α, γ) centered by the best set $(\alpha * 1.0, \gamma * 1.0)$. X- and y-axis are multiplier of α and γ used respectively in different runs.

The Cryosphere Discuss., https://doi.org/10.5194/tc-2019-7
Manuscript under review for journal The Cryosphere
Discussion started: 29 January 2019

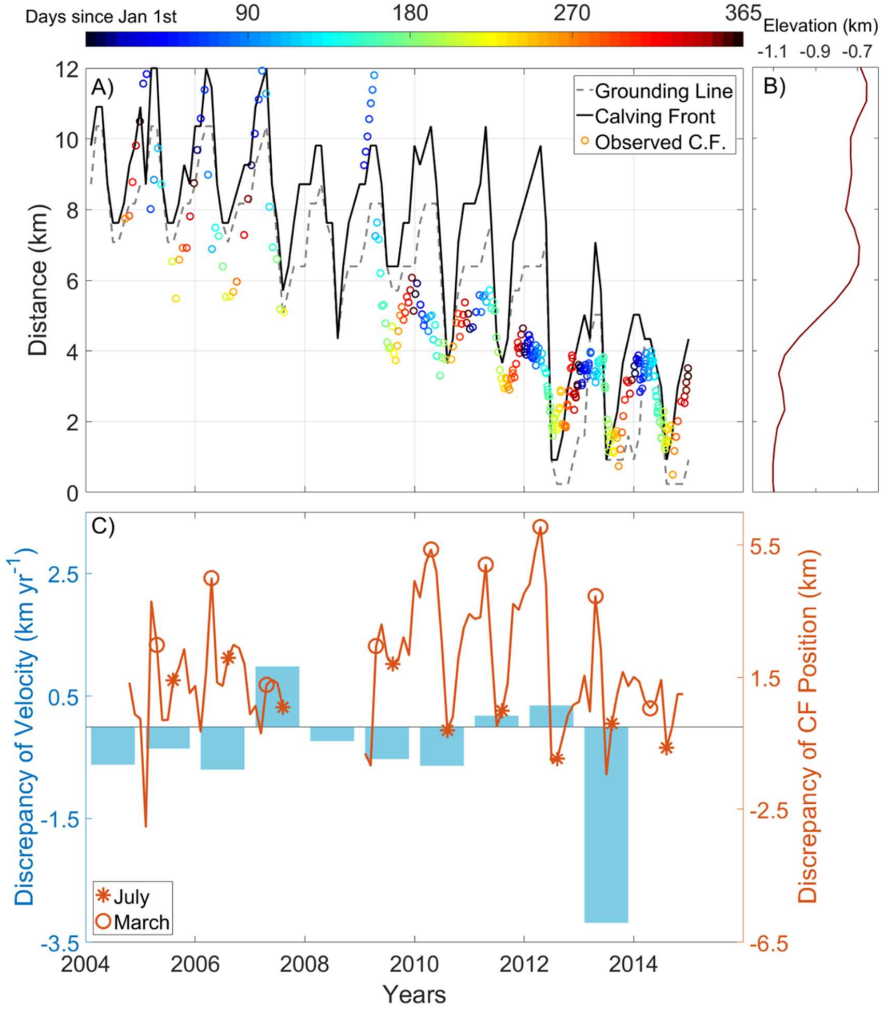

Figure 5. (A) Modeled retreat of the calving front (black solid line), grounding line (gray dashed line), and observed calving front positions (color-coded circles and scale bar) from Joughin et al. (2014). (B) Bedrock elevations. (C) Residuals (modeled minus observed) of annual mean front velocity (blue bars, left axis) and of calving front position (red lines, right axis) with typical timings of annual maximum (March) and minimum (July) extent marked. The modeled front velocities and calving positions explain about 49% and 76% of the variance

The Cryosphere Discuss., https://doi.org/10.5194/tc-2019-7
Manuscript under review for journal The Cryosphere
Discussion started: 29 January 2019

in corresponding observations.

The two biggest mismatches occur with the 2007 and especially 2013 velocities (Fig. 5). 2013 has the lowest simulated surface water run-off (Fig. 2) of all the years since 2004. The Benn calving model we use is sensitive to runoff, with reduced run-off leading to lower crevasse-penetration-depth and reduced terminus fracturing thus increasing its buttressing force. In the 2012/13 winter, the modeled glacier had an unprecedentedly high calving front and had been flowing fast the previous summer. This led to growth of an unusually long seasonal ice-shelf in the winter which caused low velocities near the end of front advancing season, and so accordingly low annual mean velocity. The low modeled velocity in 2009 can also be interpreted by the same over-growth effect, even though the ocean temperatures were high in 2009. Jakobshavn Isbræ did not in fact slow down very much in 2009 and 2013 because there were calving events that are unrepresented in our model. The relevant mechanisms are discussed later.

In 2007 high run-off caused more simulated calving and retreat than in reality. These retreat phases reduced the buttressing and lateral drag due to shear-margin-weakening, all of which lead to excessive speed-up near the terminus.

Modeled calving front retreat is ~ 7 km in total from 2004-2014 (Fig. 5), which is consistent with observations (Joughin et al. 2014). In 2009 a dramatic retreat brought the grounding line to the bottom of the bedrock slope, and since then it has gradually retreated with smaller seasonal fluctuations. The run-off forcing we applied triggered major retreats in the summers of 2007 and 2012, due to large summer peak run-off (Fig. 2), demonstrating the sensitivity of our calving parameterization to run-off forcing. Modeled timings of maximum extent and minimum extent each year are in good agreement with observations, also demonstrating that summer, in particular, May to July, run-off determines much of the behavior of Jakobshavn Isbræ.

The Cryosphere Discuss., https://doi.org/10.5194/tc-2019-7
Manuscript under review for journal The Cryosphere
Discussion started: 29 January 2019

296 The modeled range of seasonal fluctuation in front position is ~ 5 km, which is similar to
297 observations in the period before 2008. From January 2009 to December 2011, there was an abrupt
298 decrease in seasonal front fluctuation, with many winter calving events occurring, in contrast with
299 previous years (Cassotto et al. 2015). These winter calving events may explain the small observed
300 seasonal fluctuations because they limit the winter advance. Our model is unable to stimulate these
301 winter calving because there is no winter run-off, and hence calving is zero then. The largest
302 discrepancy of front position occurs during these winter calving periods (Fig. 5). Observations also
303 showed that from 2013 to 2017, Jakobshavn Isbræ barely retreated (Joughin et al. 2010). The decline
304 of run-off (Fig. 2) in 2014 suggests the reason. But since no RACMO run-off simulations are yet
305 available for 2015 and later, our parameterizations cannot be tested against this lack of retreat.

306 # 3 Future evolution

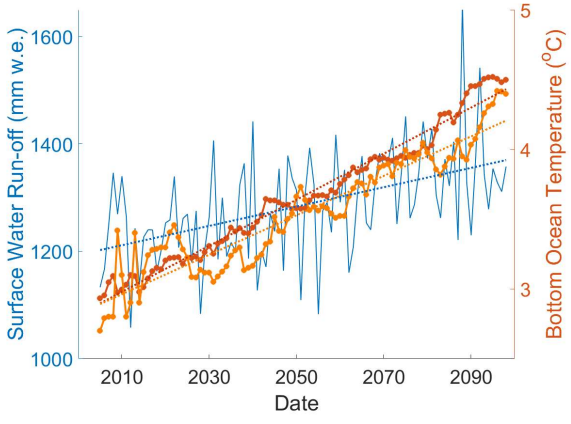

307 **Figure 6. Climate forcing for future projection under the RCP4.5 scenario taken as 300 m**
308 **depth ocean temperatures from HadGEM2-ES (orange) compared with the ensemble mean**
309 **(red) of 7 Earth System Models (HadGEM2-ES, BNU-ESM, MIROC-ESM, IPSL-CM5A-LR,**
310 **CSIRO-Mk3L-1-2, NorESM1-M and MPI-ESM-LR), (right axis), with their linear trends.**

The Cryosphere Discuss., https://doi.org/10.5194/tc-2019-7
Manuscript under review for journal The Cryosphere
Discussion started: 29 January 2019

311 **Annual maximum monthly surface water run-off near Jakobshavn Isbrae's terminus from**
312 **RACMO is shown in blue.**

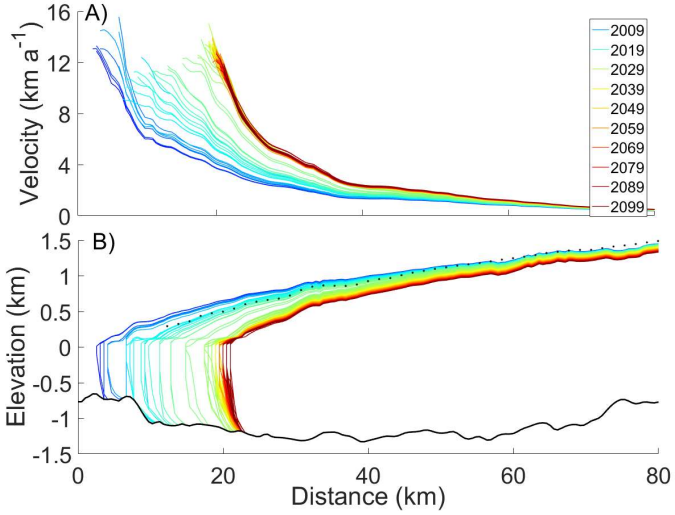

313 **Figure 7. Modeled profiles of (A) January velocity and (B) January surface elevation along**
314 **the center-flow-line of Jakobshavn Isbræ from 2004 to 2099 for the RCP4.5 scenario. Bedrock**
315 **elevation is shown in black. Black dotted line is the surface elevation profile extracted from**
316 **radar data measured around 2010 (Gogineni et al., 2012). Profiles are shown at intervals of 1**
317 **years. Profiles are color-coded in the legend and range from blue to green and red.**

318 Under the RCP4.5 scenario (Fig. 6) surface runoff slowly rises over the 21st century, with RACMO
319 simulating slightly greater runoff during the second half than for the first 50 years. Runoff increases
320 by 14% over the century. Bottom ocean temperature in the grid cell closest to Jacobshavn increases
321 by 52%, and, as may be expected, has less variability than runoff.

322 Under this forcing, Jakobshavn Isbræ continues its retreat (Fig. 7) for 18 years after 2013, producing
323 a total grounding line retreat of ~18 km upstream. As calving produces a steepening surface profile,
324 terminus velocities increase, to reach a 21st century peak of ~19 km a^{-1} in 2031 summer. Eventually
325 the calving front becomes higher than the crevasse penetration depth in the calving parameterization.

326 This leads to a stable period with little inter-annual retreat and which lasts until the end of this
327 century. During this period, nearly all of the seasonal retreats are offset by the following winter re-
328 advances. Mass transport continually flattens and thins the ice geometry, leading to reduced flow
329 speeds that eventually become half those of 2031, the 21st century peak.

330 The surprisingly high run-off anomaly in 2088 (Fig. 6) does not affect the stable state indicating
331 run-off fluctuation alone cannot break this retreat pattern immediately. Once the inter-annual retreats
332 cease in 2031, the dynamic thinning rate is greatly reduced because calving front height stops
333 increasing.

334 **Table 1 Estimates of glacier mass loss and grounding line retreat from different sources.**

Source	Climate scenario	Mass loss 2004-2013 (10 years) (Gt)	Mass loss by 2100 (Gt)	Grounding line retreat 2004-2013 (km)	Grounding line retreat by 2100 (km)
This paper	RCP4.5	234	2068 (2044-2723)	7.0	18.5 (17.5-23.0)
Muresan et al. (2016)		220			
Nick et al. (2011)	A1B		1870 - 2281		14.0 - 26.0
Observations		225±15		7.0	

335 Table 1 shows estimates of glacier mass loss and retreat. Under RCP4.5, total cumulative mass
336 change of Jakobshavn Isbræ is 2029 Gt by 2100, using best set of α, β and γ with ocean temperature
337 inputs from ensemble mean of 7 ESMs (Fig. 6). To estimate an upper bound for mass loss over this
338 century, we scale the α parameter by 1.2 giving 2680 Gt for the same forcing. Using the HadGEM2-
339 ES forcing, which is the same model used to force RACMO with α and γ set to their best estimates
340 (Fig. 4) gives 2000 Gt. We suggest that this may be the lower reasonable bound of mass loss since
341 the HadGEM-ES ocean temperatures rise notably slower than the ensemble mean.

342 Exploring the (α, γ) parameter space we notice that values of (1.0, 0.8) produces a mass loss over
343 this century of 2021 Gt with the HadGEM-ES ocean forcing, almost the same value as for the best

set of parameters. This implies that less submarine melting (determined by γ) leads to larger ice loss by dynamic processes. The reason is that lesser submarine melt allows a larger ice thickness at the grounding line with stronger dynamic thinning in advancing season. Notice in our stress balance equation (Eq. 3), thickness contributes to driving force term, thus ice flux across the grounding line is highly nonlinear in ice thickness. This highly nonlinear relationship is also shown in our sensitivity tests (Fig. 4). Over the mismatch field measured by front velocity (Fig. 4, Panel B), the velocity is partly dominated by low values of γ around the line $\alpha = 1.06$, while α is almost the only control on velocity over the region where $\alpha<1.09$. Within our sample space, the non-linear and non-monotonic relationship between submarine melting and retreats is clear (Fig. 4, Panel A). Around the point ($\alpha = 1.12$, $\gamma = 1.0$), total retreat will increase no matter if γ is decreasing or increasing within the range $0.8 < \gamma < 1.2$. The area $\alpha > 1.0$ in sample space is the very likely future condition for Jakobshavn Isbræ because increasing terminal ice cliff height caused by retreating into deep water will act as an amplifier to frontal driving force.

4 Discussion

4.1 Parameterization of Buttressing effect

The sudden 1.1℃ rise in temperature of water entering Ilulissat fjord in 1997 (Holland et al., 2008) initiated rapid melting and disintegration of the floating ice mélange in 2003. This disintegration coincided with a near doubling of ice velocities. Modeling (Vieli et al., 2011) suggested that this was due to the reduction in buttressing from the floating ice-mélange. We can realistically reproduce the velocity variation of Jakobshavn Isbræ on seasonal and inter-annual scales using our parameterization of the buttressing effect from the ice mélange in the fjord.

Gladish et al. (2015) analyzed glacial flow speeds from 1998 to 2014, finding no correlation with Ilulissat fjord temperatures. This is because at the beginning of 2004, Jakobshavn's evolution entered a new phase with the disintegration of the ice mélange and floating ice shelf. We find good correlations between Disko Bay temperatures and ice velocities from 2004 to 2014. The improvement in correlation with temperatures may be explained by a faster response between the grounded glacier and the fjord water temperatures after loss of the floating ice shelf. Thus only freshly calved icebergs played roles in providing terminus resistance, and these could be reasonably supposed to react to seasonal fjord temperatures very quickly.

Buttressing would affect the calving process by altering the longitudinal resistive stress in the glacier. Temperatures in Ilulissat Fjord will be warmer during the 21st century under essentially all climate scenarios, even those with modest emissions, due to the thermal inertia of the oceans. Thus a new floating ice shelf is unlikely to form. Prior to 2004, there were large changes in Jakobshavn: loss of ~15 km long stiff ice mélange and the sudden rise in fjord temperatures in 1998. There are fewer mechanisms to effect such dramatic changes in the future now that almost the entirety of the glacier is grounded. We therefore propose that our representation of the mélange buttressing mechanism, tuned for 2004-2013, is likely to maintain its validity during the 21st century.

4.2 Horizontal shearing and viscosity

Van Der Veen et al. (2011) estimated a maximum horizontal shear stress of ~800 kPa across the shear margin of Jakobshavn Isbræ where the horizontal velocity shear reaches the peak, while the bed stress is only 10-40 kPa in fast flowing regions (Shapero et al., 2016). Given that the width of the Jakobshavn Isbræ fast flow region is typically under 5 km and its thickness is typically between 1-2 km, these numbers indicate that the shear margins provide at least an order of magnitude greater total resistance than the bed. Thus, the shear margin, rather than the bed of Jakobshavn Isbræ

The Cryosphere Discuss., https://doi.org/10.5194/tc-2019-7
Manuscript under review for journal The Cryosphere
Discussion started: 29 January 2019

provides most of the resistance balancing the driving force. The main trunk of Jakobshavn Isbræ exhibits considerable seasonal velocity changes, while the slow moving ice outside the shear margin has little or no seasonal cycle. This flow structure implies speed gradients perpendicular to the flow direction with large seasonal variation. These velocity shears would in turn generate large seasonal variations in effective ice viscosity (Eq. 6). This mechanism implies a positive feedback on velocity in the fast flow region: increases in the speed of fast flowing ice cause increases in horizontal shear stress across the margins, reduced viscosity, and further increased horizontal velocity shear, allowing further increase to speeds in the fast flow region. Observations show that, as the terminus retreated into deeper water, seasonal fluctuations in terminus velocity increased (Joughin et al. 2008). By 2012, the summer time peak terminus velocity was ~ 17 km a^{-1}, more than twice the wintertime minimum velocity (Joughin et al. 2014). This amplified seasonal velocity cycle was likely enhanced by the shear-margin weakening mechanism.

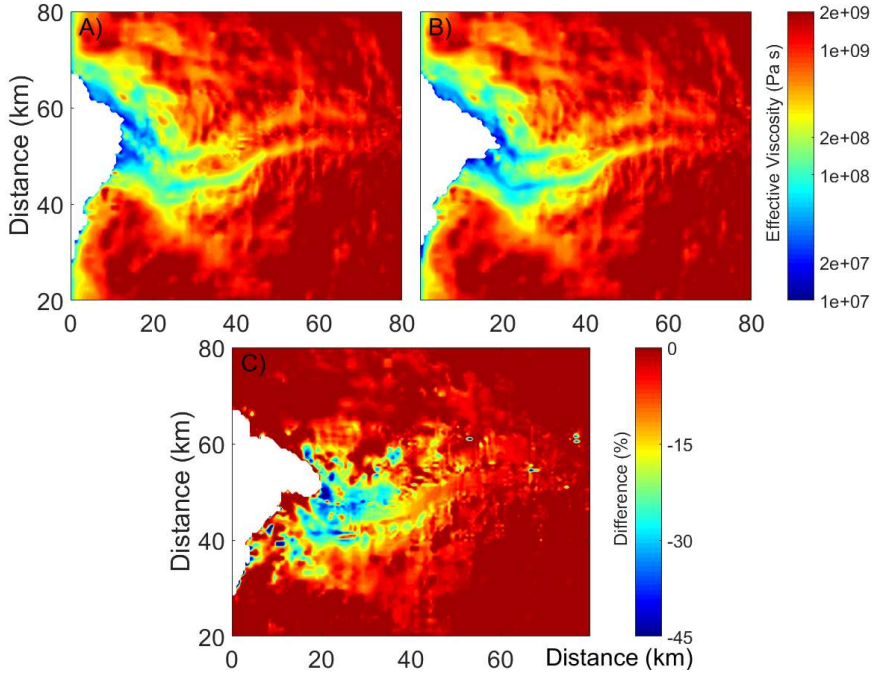

The Cryosphere Discuss., https://doi.org/10.5194/tc-2019-7
Manuscript under review for journal The Cryosphere
Discussion started: 29 January 2019

401 **Figure 8. Modeled annual mean of vertically averaged effective viscosity $\Phi\mu$ (Eq. 5) in 2004**
402 **(A) and 2013 (B) and the percentage decreases from 2004 to 2013 (C).**

403 Our modeled shear margin weakening on decadal scales is consistent with other estimates from a
404 thermomechanical ice flow model of Jakobshavn Isbræ forced by calving front positions (Bondzio
405 et al., 2017). Their modeled viscosity drops between 2003 to 2015 reach ~ 40% which is close to
406 our maximum viscosity decrease of ~ 45% between 2004 to 2013 (Fig. 8). The extreme calving
407 season we simulated in summer 2012 was accompanied by ~ 12 km a^{-1} variations in speed at the
408 calving front, which were facilitated by the accompanying shear margin-induced ice viscosity
409 reductions of 60% at the time of maximum terminus advance. Simpler models of Jakobshavn Isbræ,
410 using a flowband model (Nick et al., 2011) or simple calving parameterizations with no seasonal
411 cycle (Muresan et al., 2016) cannot produce these seasonal variations in shearing. However, our
412 model accommodates both the seasonal forcing from calving and the three-dimensional seasonal
413 velocity shear impacts on effective viscosity. Without this physical process, speedups during intense
414 calving events would be under-estimated, and this would lead to under-estimated mass
415 transportation during the retreat.

416 4.3 Comparison with previous estimates

417 The cumulative mass change of Jakobshavn Isbræ estimated from airborne and satellite laser
418 altimetry for 1997–2014 was tabulated Muresan et al. (2016). The mass loss over the 10-year period
419 2004-2013 modeled by Muresan et al. (2016) is closer to observations than ours (Table 1). This is
420 partly due to different tuning targets: matching observed mass change was a stated target in their
421 study, whereas our study targets ice front position and velocity. Their close match to observed mass
422 loss may be partly due to cancelling errors: 1) their modeled calving front barely moves after 2006,
423 which leads to under-estimation of mass change; and 2) the modeled fast flow widths are larger than

observations, which amplifies the mass flux across the calving front. These two biases will not always offset each other perfectly in the future.

Muresan et al. (2016) failed to simulate the retreat of Jakobshavn Isbræ after 2010. This may be due to the thickness threshold employed in their calving parameterization. Once Jakobshavn Isbræ terminus has retreated into the deeper part of the bedrock trough, the terminus height might never drop below their calving threshold of 375 m. In this case their calving rate will be solely due to the eigen parameterization of strain rates. Moreover, absence of seasonality in their calving front leads to under-estimated dynamic thinning, which is a key prerequisite for further calving. In contrast, our crevasse-depth calving model depends on stresses and surface water run-off with strong seasonal variation. As the terminus retreats and the surface slope steepens the enhanced surface stretching enhances the opening of crevasses in both calving parameterizations.

Nick et al. (2011) used a flow-band model to estimate a mass loss of 2280 Gt for Jakobshavn Isbræ by 2100 under the A1B climate scenario (Table 1). In our model we use RCP4.5 climate forcing, which has lower temperature rises than A1B, especially after 2050. Nick et al. (2011) prescribed a flow-band that has a near uniform width of 5 km near the terminus. Later modeling work using a similar model suggested that stability of the glacier is fundamentally controlled by geometry, and in reality the width varies along the ice-stream (Steiger et al. 2017). Nick et al. (2011) chose sets of parameters that produced small inter-annual retreats of Jakobshavn from 2000-2010, which may limit mass loss and retreat. The absence of the shear margin weakening feedback in their model also likely causes underestimation of mass loss. This could account for the comparable projected mass loss to our results, and less terminus retreat (Table 1), even though their climate forcing scenario was warmer.

The Cryosphere Discuss., https://doi.org/10.5194/tc-2019-7
Manuscript under review for journal The Cryosphere
Discussion started: 29 January 2019

4.4 Model improvements

We overestimate mass loss relative to observations over Jakobshavn Isbræ drainage basin for 2004-2013 (Table 1). The main reason is excessive dynamic thinning over the lowest ~ 20 km of the main trunk due to over-estimated summer speed. For example, modeled front velocity soared to a peak of ~ 20 km a^{-1} in summer 2012, while the observed maximum speed is only 18 km a^{-1} (Joughin et al., 2014). In this summer, we simulated a series of full-thickness calving that eventually left an unprecedented tall ice cliff. In reality, calving events do not always occur to full thickness, thus the glacier tends to form a shorter ice cliff that caters for lower velocity and less dynamic thinning.

Since the grounding line of Jakobshavn retreated to the bottom of a reverse bed slope in 2009, the height of the calving front has generally increased, causing larger mass flux downstream across the calving front. Instead of enhancing the seasonal fluctuation of calving front position, substantial winter calving events have occurred instead. Given the fact that these calving events have reduced the typical winter advance from ~ 6 km to ~ 3 km since 2010, winter calving is now likely as important as summer run-off-driven calving. During this period of low magnitude seasonal fluctuations, a series of retreats gradually moved the calving front position on inter-annual scale. In contrast, the inter-annual retreats before 2009 were mostly driven by single calving seasons, e.g., May to July 2009. Our model using the Benn calving model is better able to stimulate this earlier retreat pattern, which is largely determined by each year's peak surface water run-off.

The grounding line of Jakobshavn Isbræ is unlikely to return to shallow water in the remainder of the 21st century because bedrock elevations < - 1000 m beneath the main trunk further extend a further ~ 60 km inland. Accordingly, the latest retreat pattern including winter calving, is likely closer to the pattern of future evolution of Jakobshavn Isbræ. A short floating part due to winter calving is always accompanied by weaker lateral drag and steeper surface slope near the grounding

line, all of which are conducive for faster ice-flow. So, winter calving would enhance the downstream mass transportation, a missing process in our model.

The process of winter calving must take place without any surface water. That calving must be generated by processes affecting ice cliff stability, and that is likely due to changes at the base rather than the surface. Evidence of calving by opening of basal crevasses and splitting comes from terrestrial radar showing the terminus lifting several days prior to a large calving (Xie et al., 2016; James et al., 2014). These observations suggest that the glacier is not in hydrostatic equilibrium during calving. Our simulation specifies the glacier is in hydrostatic equilibrium on timescales of the simulation. Our model cannot simulate the process of up-lifting. Instead we assume the upper and lower surface would instantly lift to the state of floating (Eq. 1). However, there is some evidence that Jakobshavn must behave super-buoyantly in winter. We observe that the simulated grounding line of Jakobshavn retreats even after cessation of calving front retreat (Fig. 3). These retreats can be explained by rapid dynamic thinning near the grounding line leading to its buoyancy exceeding gravity and, consequently, floating.

A combination of discrete element model and continuum ice-dynamic model (solving the 3-Dimensional full-stokes equation) is able to reliably replicate observed calving styles in the case of a super-buoyant terminus (Benn et al. 2017). The discrete element model allows investigation of calving processes in unprecedented detail by analyzing the stress pattern dominated by glacier geometry and boundary conditions. However, these calving processes are beyond the capability of calving parameterization based on surface crevasse depth assuming depth-independent flow. Better understanding of this buoyancy-driven calving and further model development to represent more details such as fracture propagation are needed to accurately simulate glacier's future evolution.

The Cryosphere Discuss., https://doi.org/10.5194/tc-2019-7
Manuscript under review for journal The Cryosphere
Discussion started: 29 January 2019

5 Conclusion

We use a three-dimensional dynamic ice-sheet model with a physically-based calving parameterization to model the evolution of Jakobshavn Isbræ. After tuning the parameters, our model can accurately reproduce Jakobshavn Isbræ's retreats and velocity changes from 2004-2013 on both seasonal and inter-annual scale. We project Jakobshavn Isbræ's future dynamic changes with climate forcing data from RACMO (2014-2099) and an ensemble of 7 Earth System Models for the RCP4.5 scenario.

We successfully model two-dimensional ice-flow patterns and their seasonal variations for Jakobshavn Isbræ, which are missing from several previous modeling studies. Moreover, capturing these two-dimensional patterns allows us to handle the influence of horizontal velocity shear on effective ice viscosity, which impacts on speedup processes of Jakobshavn Isbræ.

Over most of the 21st century, Jakobshavn Isbræ's grounding line will, we predict, retreat along the deep parts of a basal trough where bedrock elevation is significantly lower than at the present grounding line. Using the current generation of calving parameterizations, which are essentially thickness threshold models, is challenging because of the increasing height of the calving front as Jakobshavn Isbræ retreats, meaning that crevasse penetration depths become too small to initiate calving. Our model successfully reproduced Jakobshavn Isbræ's retreat down a reverse bed slope with an elevation drop of ~ 400 m and the subsequent temporarily stable calving front position in 2013 and 2014.

Our results suggest that rapid dynamic thinning and calving caused by deep crevasse penetration are responsible for most of its recent mass loss, and will be a decisive process in future mass loss. Further exploration of the physics of calving and basal sliding of Greenland outlet glaciers are

513 required to improve future projections.

514 **Acknowledgements**

515 This study is supported by National Key Science Program for Global Change Research
516 (2015CB953601), National Key Research and Development Program of China (2018YFC1406104)
517 and National Natural Science Foundation of China (No. 41506212). We thank Stephen Cornford for
518 his help in implementing some parameterizations used in our model.

519

520 References

521 Alexander, P. M., and Luthcke, S. B.: Greenland Ice Sheet seasonal and spatial mass variability from
522 model simulations and GRACE (2003-2012), The Cryosphere, 10(3), 1259, 2016.

523 Amundson, J. M., Fahnestock, M., Truffer, M., Brown, J., Lüthi, M. P., and Motyka, R. J.: Ice
524 mélange dynamics and implications for terminus stability, Jakobshavn Isbræ, Greenland, J. Geophys.
525 Res.-Earth Surf., 115(F1), 2010.

526 Bamber, J. L., Layberry, R. L., and Gogineni, S. P.: A new ice thickness and bed data set for the
527 Greenland ice sheet: 1. Measurement, data reduction, and errors, J. Geophys Res.-Atmos, 106(D24),
528 33773-33780, 2001.

529 Benn, D. I., Åström, J., Zwinger, T., Todd, J., Nick, F. M., Cook, S., Hulton, N. R.J., and Luckman,
530 A.: Melt-under-cutting and buoyancy-driven calving from tidewater glaciers: new insights from
531 discrete element and continuum model simulations, J. Glaciol., 63(240), 691-702, 2017.

532 Benn, D. I., Warren, C. R., and Mottram, R. H.: Calving processes and the dynamics of calving
533 glaciers, Earth-Sci Rev., 82(3), 143-179, 2007.

534 Bentsen, M., Bethke, I., Debernard, J. B., Iversen, T., Kirkevåg, A., Seland, Ø., Drange, H., Roelandt,
535 C., Seierstad, I. A., Hoose, C., and Kristjánsson, J. E.: The Norwegian earth system model,
536 NorESM1-M-Part 1: Description and basic evaluation, Geosci. Model Dev., 5, 2843-2931, 2012.

537 Block, A. E., and Bell, R. E.: Geophysical evidence for soft bed sliding at Jakobshavn Isbrae, West
538 Greenland, The Cryosphere Discussions, 5, 339-366, 2011.

539 Bondzio, J. H., Morlighem, M., Seroussi, H., Kleiner, T., Rückamp, M., Mouginot, J., Moon, T.,
540 Larour, E. Y., and Humbert, A.: The mechanisms behind Jakobshavn Isbræ's acceleration and mass
541 loss: A 3-D thermomechanical model study, Geophys. Res. Lett., 44(12), 6252-6260, 2017.

542 Cassotto, R., Fahnestock, M., Amundson, J. M., Truffer, M., and Joughin, I.: Seasonal and
543 interannual variations in ice mélange and its impact on terminus stability, Jakobshavn Isbrae,
544 Greenland, J. Glaciol., 61(225), 76-88, 2015.

545 Collins, W. J., Bellouin, N., Doutriaux-Boucher, M., Gedney, N., Halloran, P., Hinton, T., Hughes,

546 J., Jones, C. D., Joshi, M., Liddicoat, S., Martin, G., O'Connor, F., Rae, J., Senior, C., Sitch, S.,
547 Totterdell, I., Wiltshire, A., and Martin, G.: Development and evaluation of an Earth-System model
548 HadGEM2, Geosci. Model Dev., 4(4), 1051-1075, 2011.

549 Cornford, S. L., Martin, D. F., Graves, D. T., Ranken, D. F., Le Brocq, A. M., Gladstone, R. M.,
550 Payne, A., J., Ng, E. G., and Lipscomb, W. H.: Adaptive mesh, finite volume modeling of marine
551 ice sheets, J. Comput. Phys., 232(1), 529-549, 2013.

552 Cornford, S. L., Martin, D. F., Payne, A. J., Ng, E. G., Le Brocq, A. M., Gladstone, R. M., Edwards,
553 T. L., Shannon, S. R., Agosta, C., Van Den Broeke, M. R., Hellmer, H. H., Krinner, G., Ligtenberg,
554 S. R. M., Timmermann, R., and Hellmer, H. H.: Century-scale simulations of the response of the
555 West Antarctic Ice Sheet to a warming climate, The Cryosphere, 9, 1-22, 2015.

556 Cowton, T. R., Sole, A. J., Nienow, P. W., Slater, D. A., and Christoffersen, P.: Linear response of
557 east Greenland's tidewater glaciers to ocean/atmosphere warming, P. Natl. Acad. Sci. USA, 115(31),
558 7907-7912, 2018.

559 Csatho, B., Schenk, T., Van Der Veen, C. J., and Krabill, W. B.: Intermittent thinning of Jakobshavn
560 Isbrae, West Greenland, since the little ice age, J. Glaciol., 54(184), 131-144, 2008.

561 Cuffey, K. M., and Paterson, W. S. B.: The physics of glaciers. Academic Press, 2010.

562 Dee, D., Uppala, S., Simmons, A., Berrisford, P., Poli, P., Kobayashi, S., Andrae, U., Balmaseda,
563 M., Balsamo, G., Bauer, P., Bechtold, P., Beljaars, A. C. M., van de Berg, L., Bidlot, J., Bormann,
564 N., Delsol, C., Dragani, R., Fuentes, M., Geer, A. J., Haimberger, L., Healy, S. B., Hersbach, H.,
565 Hólm, E. V., Isaksen, L., Kållberg, P., Köhler, M., Matricardi, M., McNally, A. P., Monge-Sanz, B.
566 M., Morcrette, J. J., Park, B. K., Peubey, C., de Rosnay, P., Tavolato, C., Thépaut, J. N., and Vitart,
567 F.: The ERA-Interim reanalysis: Configuration and performance of the data assimilation system, Q.
568 J. Roy. Meteor. Soc., 137, 553–597, 2011.

569 Dufresne, J. L., Foujols, M. A., Denvil, S., Caubel, A., Marti, O., Aumont, O., Balkanski, Y., Bekki,
570 S., Bellenger, H., Benshila, R., Bony, S., Bopp, L., Braconnot, P., Brockmann, P., Cadule, P., Cheruy,
571 F., Codron, F., Cozic, A., Cugnet, D., De Noblet, N., Duvel, J. P., Eth´e, C., Fairhead, L., Fichefet,
572 T., Flavoni, S., Friedlingstein, P., Grandpeix, J. Y., Guez, L., Guilyardi, E., Hauglustaine, D.,
573 Hourdin, F., Idelkadi, A., Ghattas, J., Joussaume, S., Kageyama, M., Krinner, G., Labetoulle, S.,
574 Lahellec, A., Lefebvre, M. P., Lefevre, F., Levy, C., Li, Z. X., Lloyd, J., Lott, F., Madec, G., Mancip,
575 M., Marchand, M., Masson, S., Meurdesoif, Y., Mignot, J., Musat, I., Parouty, S., Polcher, J., Rio,
576 C., Schulz, M., Swingedouw, D., Szopa, S., Talandier, C., Terray, P., Viovy, N., and Bony, S.:
577 Climate change projections using the IPSL-CM5 Earth System Model: from CMIP3 to CMIP5,
578 Clim. Dynam., 40(9-10), 2123-2165, 2013.

579 Gagliardini, O., Passalacqua, O., and Werder, M. A.: Retroactions between Basal Hydrology and
580 Basal Sliding from Numerical Experiments. In AGU Fall Meeting Abstracts, 2014.

581 Giorgetta, M. A., Jungclaus, J., Reick, C. H., Legutke, S., Bader, J., Böttinger, M., Brovkin, V.,
582 Crueger, T., Esch, M., Fieg, K., Glushak, K., Gayler, V., Haak, H., Hollweg, H., Ilyina, T., Kinne,
583 S., Kornblueh, L., Matei, D., Mauritsen, T., Mikolajewicz, U., Mueller, W., Notz, D., Pithan, F.,
584 Raddatz, T., Rast, S., Redler, R., Roeckner, E., Schmidt, H., Schnur, R., Segschneider, J., Six,
585 Katharina D., Stockhause, M., Timmreck, C., Wegner, J., Widmann, H., Wieners, K., Claussen, M.,
586 Marotzke, J., Stevens, B., and Glushak, K.: Climate and carbon cycle changes from 1850 to 2100
587 in MPI-ESM simulations for the Coupled Model Intercomparison Project phase 5, J. Adv. Model
588 Earth Sy., 5(3), 572-597, 2013.

Gladish, C. V., Holland, D. M., Rosing-Asvid, A., Behrens, J. W., and Boje, J.: Oceanic boundary conditions for Jakobshavn Glacier. Part I: Variability and renewal of Ilulissat Icefjord waters, 2001-14, J. Phys. Oceanogr., 45(1), 3-32, 2015.

Gogineni, P.: CReSIS radar depth sounder data, Center for Remote Sensing of Ice Sheets, Lawrence, KS https://data.cresis.ku.edu, 2012.

Gordon, H. B., Rotstayn, L. D., McGregor, J. L., Dix, M. R., Kowalczyk, E. A., O'Farrell, S. P., Waterman, L. J., Hirst, A. C., Wilson, S. G., Collier, M. A., and Watterson, I. G.: The CSIRO Mk3 climate system model, 2002.

Habermann, M., Truffer, M., and Maxwell, D.: Changing basal conditions during the speed-up of Jakobshavn Isbræ, Greenland, The Cryosphere, 7(6), 1679-1692, 2013.

Holland, D. M., Thomas, R. H., De Young, B., Ribergaard, M. H., and Lyberth, B.: Acceleration of Jakobshavn Isbrae triggered by warm subsurface ocean waters, Nat. Geosci., 1(10), 659, 2008.

Howat, I. M., Ahn, Y., Joughin, I., van den Broeke, M. R., Lenaerts, J. T., and Smith, B.: Mass balance of Greenland's three largest outlet glaciers, 2000-2010, Geophys. Res. Lett., 38(12), 2011.

Jakobsson, M., Mayer, L., Coakley, B., Dowdeswell, J. A., Forbes, S., Fridman, B., Hodnesdal, H., Noormets, R., Pedersen, R., Rebesco, M., Schenke, H. W., Zarayskaya, Y., Accettella, D., Armstrong, A., Anderson, R. M., Bienhoff, P., Camerlenghi, A., Church, I., Edwards, M., Gardner, J. V., Hall, J. K., Hell, B., Hestvik, O., Kristoffersen, Y., Marcussen, C., Mohammad, R., Mosher, D., Nghiem, S. V., Pedrosa, M. T., Travaglini, P. G., and Schenke, H. W.: The international bathymetric chart of the Arctic Ocean (IBCAO) version 3.0, Geophys. Res. Lett., 39(12), 2012.

James, T. D., Murray, T., Selmes, N., Scharrer, K., and O'Leary, M.: Buoyant flexure and basal crevassing in dynamic mass loss at Helheim Glacier, Nat. Geosci., 7(8), 593-596, 2014.

Ji, D., Wang, L., Feng, J., Wu, Q., Cheng, H., Zhang, Q., Yang, J., Dong, W., Dai, Y., Gong, D., Zhang, R., Wang, X., Liu, J., Moore, J. C., Chen, D., and Zhang, R. H.: Description and basic evaluation of Beijing Normal University Earth system model (BNU-ESM) version 1, Geosci. Model Dev., 7(5), 2039-2064, 2014.

Joughin, I., Abdalati, W., and Fahnestock, M.: Large fluctuations in speed on Greenland's Jakobshavn Isbrae glacier. Nature, 432(7017), 608, 2004.

Joughin, I., Howat, I. M., Fahnestock, M., Smith, B., Krabill, W., Alley, R. B., Stern, H., and Truffer, M.: Continued evolution of Jakobshavn Isbrae following its rapid speedup, J. Geophys. Res.-Earth Surf., 113(F4), 2008.

Joughin, I., Smith, B. E., and Howat, I. M.: A complete map of Greenland ice velocity derived from satellite data collected over 20 years, J. Glaciol., 64(243), 1-11, 2018.

Joughin, I., Smith, B. E., Howat, I. M., Scambos, T., and Moon, T.: Greenland flow variability from ice-sheet-wide velocity mapping, J. Glaciol., 56(197), 415-430, 2010.

Joughin, I., Smith, B., Shean, D., and Floricioiu, D.: Brief communication: Further summer speedup of Jakobshavn Isbræ, The Cryosphere, 8, 209-214, 2014.

Krabill, W., Abdalati, W., Frederick, E., Manizade, S., Martin, C., Sonntag, J., Swift, R., Thomas, R., Wright, W., and Yungel, J.: Greenland ice sheet: High-elevation balance and peripheral thinning.

Science, 289(5478), 428-430, 2000.

Luckman, A., and Murray, T.: Seasonal variation in velocity before retreat of Jakobshavn Isbræ, Greenland, Geophys. Res. Lett., 32(8), 2005.

Moss, R. H., Edmonds, J. A., Hibbard, K. A., Manning, M. R., Rose, S. K., Van Vuuren, D. P., Carter, T. R., Emori, S., Kainuma, M., Kram, T., Meehl, G. A., Mitchell, J. F.B., Nakicenovic, N., Riahi, K., Smith, S. J., Stouffer, R. J., Thomson, A. M., Weyant, J. P., and Wilbanks, T. J.: The next generation of scenarios for climate change research and assessment. Nature, 463(7282), 747-756, 2010.

Motyka, R. J., Truffer, M., Fahnestock, M., Mortensen, J., Rysgaard, S., and Howat, I.: Submarine melting of the 1985 Jakobshavn Isbræ floating mélange and the triggering of the current retreat, J. Geophys. Res.-Earth Surf., 116(F1), 2011.

Muresan, I. S., Khan, S. A., Aschwanden, A., Khroulev, C., Van Dam, T., Bamber, J., Van Den Broeke, M. R., Wouters, B., Munneke, P. K., and Kjær, K. H.: Modelled glacier dynamics over the last quarter of a century at Jakobshavn Isbræ, The Cryosphere, 10(2), 597-611, 2016.

Nick, F. M., Vieli, A., Andersen, M. L., Joughin, I., Payne, A., Edwards, T. L., Pattyn, F. and van de Wal, R. S.: Future sea-level rise from Greenland's main outlet glaciers in a warming climate. Nature, 497(7448), 235, 2013.

Pollard, D., and DeConto, R. M.: Description of a hybrid ice sheet-shelf model, and application to Antarctica, Geosci. Model Dev., 5(5), 1273, 2012.

Schoof, C., and Hindmarsh, R. C.: Thin-film flows with wall slip: an asymptotic analysis of higher order glacier flow models, Q. J. Mech. Appl. Math., 63(1), 73-114, 2010.

Shapero, D. R., Joughin, I. R., Poinar, K., Morlighem, M., and Gillet-Chaulet, F.: Basal resistance for three of the largest Greenland outlet glaciers, J. Geophys. Res.-Earth Surf., 121(1), 168-180, 2016.

Sohn, H. G., Jezek, K. C., and van der Veen, C. J.: Jakobshavn Glacier, West Greenland: 30 years of spaceborne observations, Geophys. Res. Lett., 25(14), 2699-2702, 1998.

Steiger, N., Nisancioglu, K. H., Åkesson, H., Fleurian, B. D., and Nick, F. M.: Simulated retreat of Jakobshavn Isbræ since the Little Ice Age controlled by geometry, The Cryosphere, 12(7), 2249-2266, 2018.

Tsai, V. C., Stewart, A. L., and Thompson, A. F.: Marine ice-sheet profiles and stability under Coulomb basal conditions, J. Glaciol., 61(226), 205-215, 2015.

Van Angelen, J. H., M Lenaerts, J. T., Van den Broeke, M. R., Fettweis, X., and Meijgaard, E.: Rapid loss of firn pore space accelerates 21st century Greenland mass loss, Geophys. Res. Lett., 40(10), 2109-2113, 2013.

Van Der Veen, C. J., Plummer, J. C., and Stearns, L. A.: Controls on the recent speed-up of Jakobshavn Isbræ, West Greenland, J. Glaciol., 57(204), 770-782, 2011.

Vieli, A., and Nick, F. M.: Understanding and modelling rapid dynamic changes of tidewater outlet glaciers: issues and implications, Surv. Geophys., 32(4-5), 437-458, 2011.

666 Watanabe, S., Hajima, T., Sudo, K., Nagashima, T., Takemura, T., Okajima, H., Nozawa, T., Kawase,
667 H., Abe, M., Yokohata, T., Ise, T., Sato, H., Kato. E., Takata, K., Emori, S., and Kawamiya, M.:
668 MIROC-ESM 2010: Model description and basic results of CMIP5-20c3m experiments, Geosci.
669 Model Dev., 4(4), 845, 2011.

670 Xie, S., Dixon, T. H., Voytenko, D., Holland, D. M., Holland, D., and Zheng, T.: Precursor motion
671 to iceberg calving at Jakobshavn Isbræ, Greenland, observed with terrestrial radar interferometry, J.
672 Glaciol., 62(236), 1134-1142, 2016.

673